Chapter 3

The mathematical study of an Edge crack in two different specified models under time-harmonic wave disturbance

3.1 Introduction

Composite materials have a massive significance in building mechanical structures. The materials are lighter and more sustainable as these are formed by combining two or more materials with the same or different physical properties. Due to which it generates flexibility, durability, ability to sustain heavy loads and makes it cost-efficient for production. Composites are highly involved in automobiles, aircraft, bullet trains, laminates, bridges, and many other mechanical structures. The failure in composites is a major concern for researchers and scientists. There are many causes for material failure, but in this chapter, we address failure due to fractures caused by internal and external cracks, specifically edge cracks. The problem of edge cracks in the composite medium is very challenging and is actively pursued by many researchers around the globe. Most of the aerospace industry is seeking out fiber-reinforced composite as an alternative for constructing aircraft because these are lighter, sustain heavy loads, and offer greater flexibility. Composites have a wide range of applications, from home appliances to building space crafts.

Edge cracks are the more catastrophic type of cracks because these are more vulnerable than interior cracks. Dealing with edge cracks can be challenging as these are found more often in our day-to-day life, and fracture tendency is higher, and the possibility of crack arrest is lower. Scientists, engineers, and researchers are dealing

with edge cracks for the last few decades, and still, these types of cracks are as challenging as new. To deal with edge cracks, SIF plays a very crucial role. It is evident from the literature survey many scientists and researchers have contributed to the edge crack problems in the composite and orthotropic media as Sneddon and Das [78] have studied the SIF for an edge crack situated in an elastic half-plane, further studied by Achenbach et al. [79] in an elastodynamic medium while Gupta and Erdogan [80] have investigated some edge crack problems in an infinite strip. Hasebe and Inohara [81] did the stress analysis of a semi-infinite plate with an oblique edge crack. Afterward, edge crack for thermal loading in a nonhomogeneous half-plane has been studied by Jin and Noda [82], furthermore transient loading stress for an edge crack analyzed by JIN and Paulio [83] and Guo et al. [84] studied the dynamical response in a functionally graded orthotropic strip of an edge crack. Das et al. [85] [86] [87] [88] have derived the SIF for an edge crack that is bonded in orthotropic material. Chiu et al. [89]have derived the scattering effect of the edge-guided wave by an edge crack. Lee and Beom [90] contributed a study about an interfacial edge crack between dissimilar orthotropic materials.

A broad number of studies have been conducted and still going on for composite materials and their benefits for the betterment of humankind and to save human resources. Whitworth [91] provided modeling stiffness reduction of graphite/epoxy composite laminate [92] [93] [94], which helped aerospace industries. Naik et al. [95] derived high strain rate tensile behavior of e-glass epoxy composites. Jia [96] studied for enhancement of ablative and interfacial bonding properties of EPDM composites, while Linganiso and Anandjiwala [97] studies fiber-reinforced laminates in aerospace engineering to reduce the weight of the overall model. Recently, Miao and Tippur [98] have studied the effect of loading rate on fracture behavior of carbon fiber reinforced polymer composites. Afterward, Yuhazri et al. [99] explores its strengthening for a concrete structure. Xu et al. [100] studied weight function method for orthotropic single edge notched specimen, and Petrova and Schmauder [101] have studied a theoretical model with a system of edge crack and internal cracks. Whereas Itou [102] studied the time-harmonic wave disturbance on three collinear cracks.

When we work in the actual world, the surfaces of the system are open to all types of waves and pressure present in our environment, disturbing the system body and its related components. Wave disturbances are the main disturbance caused by the environment; for example, the pressure on aircraft while flying causes light and compression waves. The time-harmonic wave disturbances are caused by impinging the time-harmonic waves on the surface, which creates pressure on the crack surface. Due to this, the crack surface got affected, which leads to affect the speed of crack

propagation and the stress field around the crack.

The present study proposes two mathematical edge cracked models, in which problem-1 consists of an edge crack in a semi-infinite orthotropic strip of finite depth h bonded by orthotropic half-plane.While the problem-2 consists of the edge crack is situated in a vertical semi-infinite orthotropic strip of depth h. The problems are solved by applying Fourier transformation technique to get the pair of integral equations, and the unknowns were obtained by using the Schmidt method [103]. Approximate analytical expression of stress intensity factor under time-harmonic wave disturbance at the tip of the edge crack has been derived. The graphical representations of SIF for variations of wave numbers and crack lengths with respect to various depths of the strip have been shown for both the problems. A comparison of the study of SIFs of edge crack for the problems is the salient feature of this chapter.

3.2 Mathematical formulation

Consider an edge crack of finite length $(0 < x < a)$ in two different problems. For problem-1, the edge crack is situated in the orthotropic strip of finite thickness h bonded by an orthotropic half-plane (Fig.3.1). For problem-2, the edge crack is situated in the orthotropic strip of the same thickness (Fig.3.2).

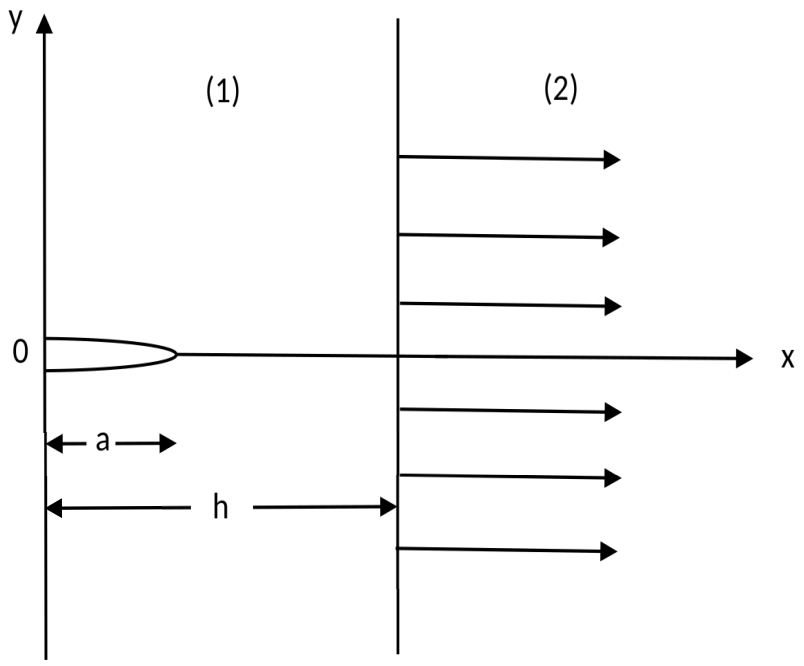

Figure 3.1: The crack geometry of Problem-1

The displacement equations for both the problems are given by

$$C_{11}^{(j)}\frac{\partial^2 u^{(j)}}{\partial x^2}+\frac{\partial^2 u^{(j)}}{\partial y^2}+\left(1+C_{12}^{(j)}\right)\frac{\partial^2 v^{(j)}}{\partial x\partial y}+\frac{\omega^2}{C_T^{(j)2}}u^{(j)}=0, \tag{3.2.1}$$

$$\frac{\partial^2 v^{(j)}}{\partial x^2}+C_{22}^{(j)}\frac{\partial^2 v^{(j)}}{\partial y^2}+\left(1+C_{12}^{(j)}\right)\frac{\partial^2 u^{(j)}}{\partial x\partial y}+\frac{\omega^2}{C_T^{(j)2}}v^{(j)}=0, \tag{3.2.2}$$

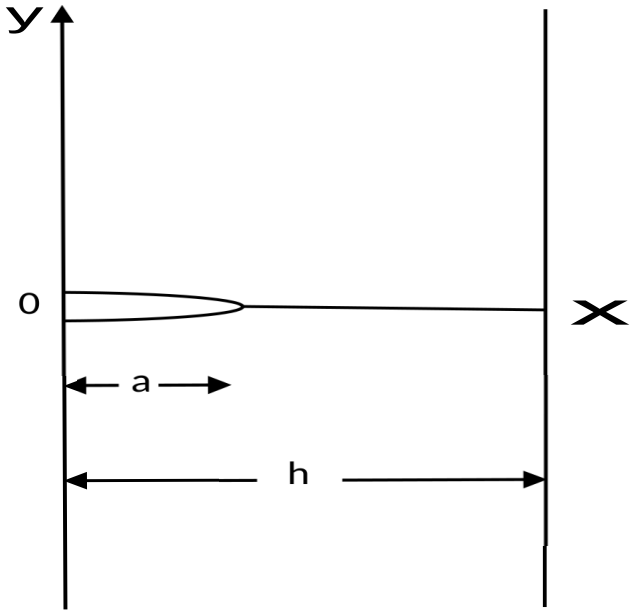

Figure 3.2: The crack geometry of Problem-2

where $C_{ik}^{(j)}$'s are the elastic constants, and the superscripts $j = 1, 2$ refer to medium 1 and medium 2, respectively. The corresponding stresses are given by

$$\sigma_{xx}^{(j)}=C_{66}^{(j)}\left(C_{11}^{(j)}\frac{\partial u^{(j)}}{\partial x}+C_{12}^{(j)}\frac{\partial v^{(j)}}{\partial y}\right), \tag{3.2.3}$$

$$\sigma_{yy}^{(j)}=C_{66}^{(j)}\left(C_{12}^{(j)}\frac{\partial u^{(j)}}{\partial x}+C_{22}^{(j)}\frac{\partial v^{(j)}}{\partial y}\right), \tag{3.2.4}$$

$$\sigma_{xy}^{(j)}=C_{66}^{(j)}(\frac{\partial u^{(j)}}{\partial y}+\frac{\partial v^{(j)}}{\partial x}). \tag{3.2.5}$$

Consider incident elastic waves that move along the y-axis in the negative direction. the corresponding displacements are found as

$u^{(j)}=0$

$v^{(j)} = \varepsilon_v exp[i\omega y/C_T^{(j)}\sqrt{C_{22}^{(j)}}]$

The common boundary conditions for both the problems are as follows:

On $y = 0$,

$$\sigma_{yy}^{(1)}(x,0) = -p, \qquad 0 \le x \le a, \tag{3.2.6}$$

$$\sigma_{xy}^{(1)}(x,0) = 0, \qquad 0 \le x \le h, \tag{3.2.7}$$

$$v^{(1)}(x,0) = 0, \qquad a < x < h, . \tag{3.2.8}$$

On the boundary $x = 0$,

$$\sigma_{xx}^{(1)}(0,y) = 0, \qquad |y| < \infty, \tag{3.2.9}$$

$$\sigma_{xy}^{(1)}(0,y) = 0, \qquad |y| < \infty, \tag{3.2.10}$$

Continuity conditions on the interface position $x = h$, for problem-1 are as follows

$$u^{(1)}(h,y) = u^{(2)}(h,y), \qquad |y| < \infty, \tag{3.2.11}$$

$$v^{(1)}(h,y) = v^{(2)}(h,y), \qquad |y| < \infty, \tag{3.2.12}$$

$$\sigma_{yy}^{(1)}(h,y) = \sigma_{yy}^{(2)}(h,y), \qquad |y| < \infty, \tag{3.2.13}$$

$$\sigma_{xy}^{(1)}(h,y) = \sigma_{xy}^{(2)}(h,y), \qquad |y| < \infty, \tag{3.2.14}$$

boundary conditions on the position $x = h$, for problem-2 are as follows

$$\sigma_{xx}^{(1)}(h,y) = 0, \qquad |y| < \infty, \tag{3.2.15}$$

$$\sigma_{xy}^{(1)}(h,y) = 0, \qquad |y| < \infty, \tag{3.2.16}$$

The stress components vanish from the remote distance of the crack.

3.3 Solution of the problems

Applying the Fourier transformation Eq.(1.4.1) on Eq.(3.2.1) , we get

$$\left(\frac{d^4}{dy^4} + q\frac{d^2}{dy^2} + r\right)(\overline{u_i},\, \overline{v_i}) = 0, \tag{3.3.1}$$

where

$$q_j = \zeta^2(2C_{12}^{(j)} - C_{11}^{(j)}C_{12}^{(j)} + C_{12}^{(j)2})/C_{22}^{(j)} + (1 + C_{22}^{(j)})\frac{\omega^2}{C_{22}^{(j)}C_T^{(j)2}},$$

$$r_j = \left(\zeta^2 C_{11}^{(j)} - \frac{\omega^2}{C_T^{(j)2}}\right)\left(\zeta^2 - \frac{\omega^2}{C_T^{(j)2}}\right)/C_{22}^{(j)} \tag{3.3.2}$$

Expressions of the solution can be assumed as

$$\begin{aligned}\overline{u}^{(1)}(\xi,\, y) &= A^{(1)}(\xi)\exp(\gamma_1^{(1)}y) + B^{(1)}(\xi)\exp(-\gamma_1^{(1)}y)\cosh(\gamma_1^{(1)}\xi)\\ &\quad + C^{(1)}(\xi)\exp(\gamma_2^{(1)}y) + D^{(1)}(\xi)\exp(-\gamma_2^{(1)}y)\cosh(\gamma_2^{(1)}\xi),\end{aligned} \tag{3.3.3}$$

$$\begin{aligned}\overline{v}^{(1)}(\xi,\, y) &= \alpha_1^{(1)}A^{(1)}(\xi)\exp(\gamma_1^{(1)}y) - \alpha_1^{(1)}B^{(1)}(\xi)\exp(-\gamma_1^{(1)}y)\cosh(\gamma_1^{(1)}\xi)\\ &\quad + \alpha_2^{(1)}C^{(1)}(\xi)\exp(\gamma_2^{(1)}y) - \alpha_2^{(1)}D^{(1)}(\xi)\exp(-\gamma_2^{(1)}y)\cosh(\gamma_2^{(1)}\xi),\end{aligned} \tag{3.3.4}$$

$$\begin{aligned}\overline{u}^{(2)}(\xi,\, y) &= A^{(2)}(\xi)\exp(-\gamma_1^{(2)}\xi)\cosh(\gamma_1^{(2)}y)\\ &\quad + B^{(2)}(\xi)\exp(-\gamma_2^{(2)}\xi)\cosh(\gamma_2^{(2)}y),\end{aligned} \tag{3.3.5}$$

$$\begin{aligned}\overline{v}^{(2)}(\xi,\, y) &= -\alpha_1^{(2)}A^{(2)}(\xi)\exp(-\gamma_1^{(2)}\xi)\cosh(\gamma_1^{(2)}y)\\ &\quad - \alpha_1^{(2)}B^{(2)}(\xi)\exp(-\gamma_2^{(2)}\xi)\cosh(\gamma_2^{(2)}y),\end{aligned} \tag{3.3.6}$$

where $\gamma_k^{(j)}$'s are the roots of the Eq.(3.3.1) and $\alpha_k^{(j)} = \left(\frac{\gamma_k^{(j)} - \zeta^2 C_{11}^{(j)}/\gamma_k^{(j)} + \omega^2/(C_T^{(j)2}\gamma_k^{(j)})}{i\zeta(1+C_{12}^{(j)})}\right)$, $k = 1,\, 2;\ j = 1,\, 2.$

The expressions for stresses are obtained as

$$\begin{aligned}\overline{\sigma}_{yy}^{(1)}(\xi, y)\setminus C_{66}^{(1)} &= i\xi C_{12}^{(1)}((A^{(1)}\exp(\gamma_1^{(1)}y)+B^{(1)}\exp(-\gamma_1^{(1)}y)\cosh(\gamma_1^{(1)}\xi)\\ &+C^{(1)}\exp(\gamma_2^{(1)}y))+D^{(1)}\exp(-\gamma_2^{(1)}y)\cosh(\gamma_2^{(1)}\xi)\\ &+C_{22}^{(1)}(\alpha_1^{(1)}\gamma_1^{(1)}(A^{(1)}\exp(\gamma_1^{(1)}y)+B^{(1)}\exp(-\gamma_1^{(1)}y)\cosh(\gamma_1^{(1)}\xi))\\ &+\alpha_2^{(1)}\gamma_2^{(1)}(C^{(1)}\exp(\gamma_2^{(1)}y)+D^{(1)}\exp(-\gamma_2^{(1)}y)\cosh(\gamma_2^{(1)}\xi)),\end{aligned} \tag{3.3.7}$$

$$\begin{aligned}\overline{\sigma}_{xy}^{(1)}(\xi, y)\setminus C_{66}^{(1)} &= (\gamma_1^{(1)}(A^{(1)}\exp(\gamma_1^{(1)}y)-B^{(1)}\exp(-\gamma_1^{(1)}y)\cosh(\gamma_1^{(1)}\xi))\\ &+\gamma_2^{(1)}(C^{(1)}\exp(\gamma_2^{(1)}y)-D^{(1)}\exp(-\gamma_2^{(1)}y)\cosh(\gamma_2^{(1)}\xi))\\ &+i\xi(\alpha_1^{(1)}A^{(1)}\exp(\gamma_1^{(1)}y)-\alpha_1^{(1)}B^{(1)}\exp(-\gamma_1^{(1)}y)\cosh(\gamma_1^{(1)}\xi)\\ &+\alpha_2^{(1)}C^{(1)}\exp(\gamma_2^{(1)}y)-\alpha_2^{(1)}D^{(1)}\exp(-\gamma_2^{(1)}y)\cosh(\gamma_2^{(1)}\xi)),\end{aligned} \tag{3.3.8}$$

$$\begin{aligned}\overline{\sigma}_{yy}^{(2)}(\xi, y)\setminus C_{66}^{(2)} &= i\xi C_{12}^{(2)}(A^{(2)}\exp(-\gamma_1^{(2)}y)\cosh(\gamma_1^{(2)}\xi)\\ &+B^{(2)}\exp(-\gamma_2^{(2)}y)\cosh(\gamma_2^{(2)}\xi))\\ &+C_{22}^{(2)}(\alpha_1^{(2)}\gamma_1^{(2)}A^{(2)}\exp(-\gamma_1^{(2)}y)\cosh(\gamma_1^{(2)}\xi)\\ &+\alpha_2^{(2)}\gamma_2^{(2)}B^{(2)}\exp(-\gamma_2^{(2)}y)\cosh(\gamma_2^{(2)}\xi)),\end{aligned} \tag{3.3.9}$$

$$\begin{aligned}\overline{\sigma}_{xy}^{(2)}(\xi, y)\setminus C_{66}^{(2)} &= (-\gamma_1^{(2)}A^{(2)}\exp(-\gamma_1^{(2)}y)\cosh(\gamma_1^{(2)}\xi)\\ &-\gamma_2^{(2)}B^{(2)}\exp(-\gamma_2^{(2)}y)\cosh(\gamma_2^{(2)}\xi))\\ &+i\xi(-\alpha_1^{(2)}A^{(2)}\exp(-\gamma_1^{(2)}y)\cosh(\gamma_1^{(2)}\xi)\\ &-\alpha_2^{(2)}B^{(2)}\exp(-\gamma_2^{(2)}y)\cosh(\gamma_2^{(2)}\xi)),\end{aligned} \tag{3.3.10}$$

For problem-1, using the boundary condition (3.2.7), and (3.2.9)-(3.2.10) with the continuity conditions (3.2.11) - (3.2.14) , we get

$$\begin{aligned}B^{(1)} &= \nabla_1 A^{(1)},\\ C^{(1)} &= (\nabla_3+\nabla_2\nabla_1)A^{(1)},\\ D^{(1)} &= \nabla_4 A^{(1)},\\ A^{(2)} &= \nabla_5 A^{(1)},\\ B^{(2)} &= \nabla_6 A^{(1)},\end{aligned} \tag{3.3.11}$$

where

$$\nabla_1 = \frac{[(\gamma_1^{(1)}+i\xi\alpha_1^{(1)})+(\gamma_2^{(1)}+i\xi\alpha_2^{(1)})(\nabla_3-\beta_6\nabla_3\cosh(\gamma_2^{(2)}h))]}{[(\gamma_1^{(1)}+i\xi\alpha_1^{(1)})\cosh(\gamma_1^{(1)}h)+(\gamma_2^{(1)}+\mathrm{i}\xi\alpha_2^{(1)})(\nabla_2-(\beta_5+\beta_6\nabla_2\cosh(\gamma_2^{(1)}h))]\cosh(\gamma_1^{(1)}h)},$$

$$\nabla_2 = \frac{-(1+\beta_5-\beta_4\,\beta_5)}{(1+\beta_6-\beta_3-\beta_4\,\beta_6)},$$
$$\nabla_3 = \frac{-1}{(1+\beta_6-\beta_3-\beta_4\,\beta_6)},$$
$$\nabla_4 = \frac{\beta_5\,\nabla_1+\beta_6(\nabla_3+\nabla_2\,\nabla_1)}{\cosh(\gamma_2^{(1)}h)},$$
$$\nabla_5 = (\beta_3\nabla_1+\beta_3\nabla_2\nabla_1+\beta_4\nabla_4)\exp(\gamma_1^{(2)}h),$$
$$\beta_1 = -2\phi_6+\frac{2\phi_5\alpha_1^{(2)}}{\alpha_1^{(1)}},$$
$$\beta_2 = \phi_7+\phi_5-\frac{\phi_3(\alpha_1^{(2)}+\alpha_1^{(1)})}{\alpha_1^{(1)}}-\frac{(\phi_1-\phi_3)(\phi_6-\phi_5-(\phi_5/\alpha_1^{(1)})(\alpha_2^{(1)}-\alpha_1^{(1)}))}{(\phi_2-\phi_1)},$$
$$\beta_3 = \frac{(\phi_2-\phi_1)}{(\phi_3-\phi_1+(\phi_4/\phi_8)\beta_2)},$$
$$\beta_4 = \frac{(\phi_2-\phi_1+(\phi_4/\phi_8)\beta_1)}{(\phi_3-\phi_1+(\phi_4/\phi_8)\beta_2)},$$
$$\beta_5 = \frac{-2\alpha_1^{(1)}}{(\alpha_2^{(1)}+\alpha_1^{(1)})-(\alpha_1^{(2)}+\alpha_1^{(1)})\beta_4},$$
$$\beta_6 = \frac{(\alpha_2^{(1)}-\alpha_1^{(1)})+(\alpha_1^{(2)}+\alpha_1^{(1)})\beta_3}{(\alpha_2^{(1)}+\alpha_1^{(1)})-(\alpha_1^{(2)}+\alpha_1^{(1)})\beta_4},$$
$$\phi_1 = C_{66}^{(1)}(i\xi C_{12}^{(1)}+C_{22}^{(1)}\alpha_1^{(1)}\gamma_1^{(1)}),$$
$$\phi_2 = C_{66}^{(1)}(i\xi C_{12}^{(1)}+C_{22}^{(1)}\alpha_2^{(1)}\gamma_2^{(1)}),$$
$$\phi_3 = C_{66}^{(2)}(i\xi C_{12}^{(2)}+C_{22}^{(2)}\alpha_1^{(2)}\gamma_1^{(2)}),$$
$$\phi_4 = C_{66}^{(2)}(i\xi C_{12}^{(2)}+C_{22}^{(2)}\alpha_2^{(2)}\gamma_2^{(2)}),$$
$$\phi_5 = C_{66}^{(1)}(i\xi\alpha_1^{(1)}+\gamma_1^{(1)}),$$
$$\phi_6 = C_{66}^{(1)}(i\xi\alpha_2^{(1)}+\gamma_2^{(1)}),$$
$$\phi_7 = C_{66}^{(2)}(-i\xi\alpha_1^{(2)}-\gamma_1^{(2)}),$$
$$\phi_8 = C_{66}^{(2)}(-i\xi\alpha_2^{(2)}-\gamma_2^{(2)}),$$

For problem-2, using boundary condition (3.2.7) and the continuity conditions (3.2.15) - (3.2.16), we get

$$B^{(1)} = (f_1+f_2f_4)\,A^{(1)},$$
$$C^{(1)} = f_4A^{(1)},$$
$$D^{(1)} = f_3\,A^{(1)},$$
$$A^{(2)} = 0,$$
$$B^{(2)} = 0, \tag{3.3.12}$$

$$f_1 = \frac{\cosh(\gamma_2^{(1)}h) - 1}{\cosh(\gamma_2^{(1)}h) - \cosh(\gamma_1^{(1)}h)},$$
$$f_2 = \frac{(\gamma_2^{(1)} + i\xi\alpha_2^{(1)})(\cosh(\gamma_2^{(1)}h) - 1)}{\cosh(\gamma_2^{(1)}h) - \cosh(\gamma_1^{(1)}h)}$$
$$f_3 = \frac{-(\gamma_1^{(1)} + i\xi\alpha_1^{(1)})(\cosh(\gamma_1^{(1)}h) - 1)}{(\gamma_2^{(1)} + i\xi\alpha_2^{(1)})(\cosh(\gamma_2^{(1)}h) - 1)},$$
$$f_4 = \frac{(\gamma_1^{(1)} + i\xi\alpha_1^{(1)})(\cosh(\gamma_1^{(1)}h) - 1) + (\gamma_2^{(1)} + i\xi\alpha_2^{(1)})f_1 f_3 \cosh(\gamma_2^{(1)}h)}{f_2(\gamma_1^{(1)} + i\xi\alpha_1^{(1)})\cosh(\gamma_1^{(1)}h) + (\gamma_2^{(1)} + i\xi\alpha_2^{(1)})(1 - f_2 f_3 \cosh(\gamma_2^{(1)}h))}$$

The boundary conditions (3.2.6) and (3.2.8) with the aid of expressionss (3.3.11) and (3.3.12), we get

$$\frac{1}{\pi}\int_0^\infty \overline{v}^{(1)}(\xi, 0)R(\xi)\cos(\xi x)d\xi = -\frac{p}{C_{66}^{(1)}}, \quad 0 \le x < a, \tag{3.3.13}$$

$$\frac{1}{\pi}\int_0^\infty \overline{v}^{(1)}(\xi, 0)\cos(\xi x)d\xi, \quad a < x, \tag{3.3.14}$$

where for problem-1

$$\begin{aligned} R(\xi) = {} & [(i\xi C_{12}^{(1)} + C_{22}^{(1)}\alpha_1^{(1)}\gamma_1^{(1)})(1 + \nabla_1 \cosh(\gamma_1^{(1)}h)) \\ & + (i\xi C_{12}^{(1)} + C_{22}^{(1)}\alpha_2^{(1)}\gamma_2^{(1)})(\nabla_3 + \nabla_2\nabla_1 + \nabla_4 \cosh(\gamma_2^{(1)}h))] \\ & /[\alpha_1^{(1)}(1 - \nabla_1 \cosh(\gamma_1^{(1)}h)) + \alpha_2^{(1)}(\nabla_3 + \nabla_2\nabla_1 - \nabla_4 \cosh(\gamma_2^{(1)}h))], \\ & h > 0 \end{aligned} \tag{3.3.15}$$

for problem-2

$$\begin{aligned} R(\xi) = {} & [(i\xi C_{12}^{(1)} + C_{22}^{(1)}\alpha_1^{(1)}\gamma_1^{(1)})(1 + (f_1 + f_2 f_4)\cosh(\gamma_1^{(1)}h)) \\ & + (i\xi C_{12}^{(1)} + C_{22}^{(1)}\alpha_2^{(1)}\gamma_2^{(1)})(f_4 + (f_1 f_3 + f_1 f_2 f_4)\cosh(\gamma_2^{(1)}h))] \\ & /[\alpha_1^{(1)}(1 - (f_1 + f_2 f_4)\cosh(\gamma_1^{(1)}h)) + \alpha_2^{(1)}(f_4 - (f_1 f_3 + f_1 f_2 f_4)\cosh(\gamma_2^{(1)}h))], \\ & h > 0 \end{aligned} \tag{3.3.16}$$

Representing $v^{(1)}(x, 0)$ by the series

$$\pi C_{66}^{(1)} v^{(1)}(x,0) = \sum_{n=1}^{\infty} c_n^{(1)} \cos\{(2n-1)\sin^{-1}(x/a)\}, \quad 0 < x < a, \tag{3.3.17}$$
$$= 0, \qquad\qquad elsewhere.$$

we see that the condition (3.3.14) is satisfied. The Fourier transformation of the Eq.(3.3.17) is obtained as

$$C_{66}^{(1)} \overline{v}^{(1)}(\xi,0) = \sum_{n=1}^{\infty} c_n^{(1)} \frac{(2n-1)}{2\xi} J_{2n-1}(\xi a) \tag{3.3.18}$$

where $c_n^{(1)}$ $'s$ are the unknown coefficients to be determined and $J_{2n-1}(\xi a)$ is the Bessel function of first kind.

The expression of the normal stress is obtained as

$$\sigma_{yy}^{(1)}(x,0) = \frac{1}{\pi} \sum_{n=1}^{\infty} c_n^{(1)} (2n-1) \int_0^{\infty} \frac{R(\xi)}{\xi} J_{2n-1}(\xi a) \cos(\xi x) d\xi \tag{3.3.19}$$

In order to find the coefficients $c_n^{(1)}$ $'s$, the Schmidt method [103] is used, for which the expression (3.3.13) with the aid of expression (3.3.19) can be reduced to the following form

$$\sum_{n=1}^{\infty} c_n^{(1)} Q_n^{(1)}(x) = -p, \qquad\qquad 0 \le x < a, \tag{3.3.20}$$

where

$$Q_n^{(1)}(x) = \frac{(2n-1)}{\pi} \int_0^{\infty} \frac{R(\xi)}{\xi} J_{2n-1}(\xi a) \cos(\xi x) d\xi, \tag{3.3.21}$$

Let us construct a set of orthogonal functions $W_n(x)$ from the set of functions $Q_n^{(1)}(x)$, which satisfying the given condition of orthogonality as follows:

$$\int_0^a W_n(x) W_m(x) dx = N_n \delta_{nm}, \quad W_n(x) = \sum_{n=1}^{\infty} \frac{S_{in}}{S_{nn}} Q_i^{(1)}(x), \tag{3.3.22}$$

where $N_n = \int_0^a [W_n(x)]^2 dx$ and $W_1(x) = Q_1^{(1)}(x)$ and $S_{in}'s$ are the cofactors of the elements s_{in} of S_n as follows:

$$S_n = \begin{vmatrix} s_{11} & s_{12} & \dots & s_{1n} \\ s_{21} & s_{22} & \dots & s_{2n} \\ \vdots & \vdots & & \vdots \\ s_{n1} & s_{n2} & \dots & s_{nn} \end{vmatrix}, \qquad s_{in} = \int_0^a Q_i^{(1)}(x) Q_n^{(1)}(x) dx. \tag{3.3.23}$$

The Eq.(3.3.20) can be written in the form of orthogonal set of functions $Q_n^{(1)}(x)$ as

$$\sum_{n=1}^{\infty} c_n^{(1)} Q_n^{(1)}(x) = \sum_{n=1}^{\infty} q_n W_n(x) = -p. \tag{3.3.24}$$

using the last two equalities to get the value of q_n and using that value and first two equality to get the values of $c_n^{(1)}$ as follows:

$$c_n^{(1)} = \sum_{j=n}^{\infty} d_j \frac{S_{nj}}{S_{jj}}, \tag{3.3.25}$$

where $d_j = \frac{-1}{N_j} \int_0^a p W_j(x) dx$. For large value of ξ, the value of R^Lcan be evaluated as $R(\xi)/\xi \to R^L$, i.e.,

$$R^L = R(\xi_l)/\xi_l, \tag{3.3.26}$$

where ξ_l is considered to be very large value of ξ. Now in order to evaluate the integral in Eq.(3.3.19) , we use the following relation

$$\int_0^{\infty} J_n(xz)\cos(yz) dz = \frac{-x^n \sin(n\pi/2)}{\sqrt{y^2 - x^2}\{y + \sqrt{y^2 - x^2}\}^n}, \qquad y > x. \tag{3.3.27}$$

With the help of Eqs.(3.3.21),(3.3.26) and (3.3.27),$Q_n^{(1)}(x)$ can be expressed as

$$\begin{aligned} Q_n^{(1)}(x) = \frac{(2n-1)}{\pi} [& \int_0^{\infty} \left(R(\xi)/\xi - R^L \right) J_{2n-1}(\xi a) \cos(\xi x) d\xi \\ & + R^L [(-a)^{2n-1} \sin((2n-1)\pi/2) / [\sqrt{(x^2 - a^2)}\{x + \sqrt{(x^2 - a^2)}\}^{2n-1}]. \end{aligned} \tag{3.3.28}$$

The dynamic Mode- I stress intensity factor (K_{Ia}) for both the problems at the tip $x = a$ of the edge crack is determined as

$$K_{Ia} = \{2\pi(x-a)\}^{1/2} \lim_{x \to a^+} \sigma_{yy}^{(1)}(x, 0) = \sum_{n=1}^{\infty} c_n^{(1)} (2n-1)(-1)^n R^L / (\pi a)^{1/2}. \tag{3.3.29}$$

3.4 Results and discussion

For the numerical computation of the given mathematical models, the composite material Graphite-epoxy and E-glass epoxy are taken as vertical orthotropic strip and half-plane, respectively for Problem-1. For Problem-2, the Graphite-epoxy as the material for the orthotropic strip. The engineering material constants are given in Table-2.1 of the previous chapter.

The dimensionless dynamic mode- I SIF (K_{Ia}) for both the problems at the crack tip $x = a$ of the edge crack has been numerically calculated by using the expression in Eq.(3.3.29). The variations of the dimensionless SIF have been shown graphically for various width ($h = 2, 4\, and\, 6$) of the vertical strip for various crack lengths and wave numbers ($a\omega/C_T^{(1)}$). It can be easily determined that the SIF was higher for the smaller value of the h, i.e., when the depth of the strip is less, the SIF is higher, which shows the effect of the decrease in SIF as an increase in the depth of the strip.

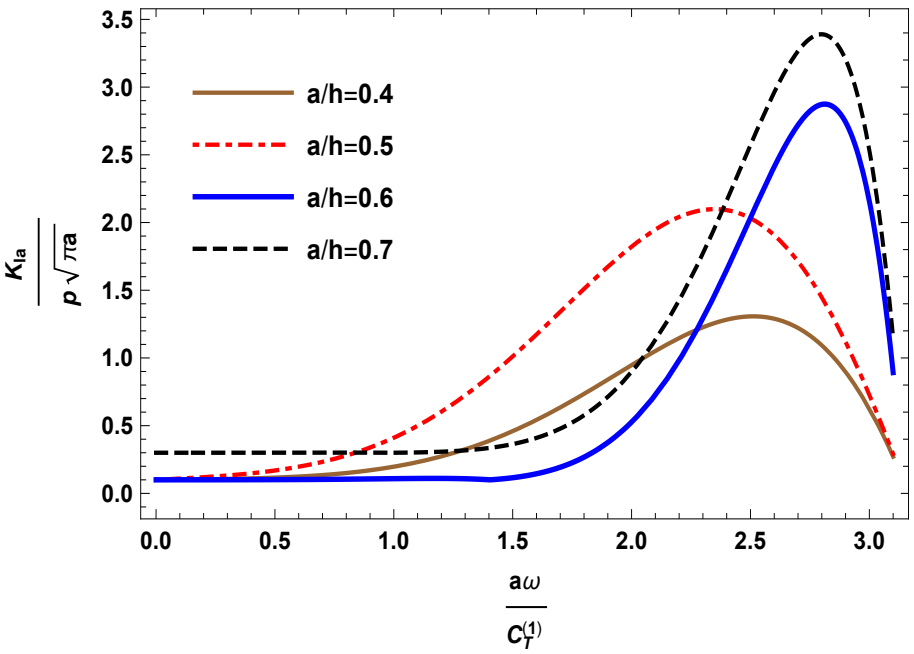

Figure 3.3: Variation of normalized K_{Ia} vs. $a\omega/C_T^{(1)}$ for problem-1 at $a/h = 0.4, 0.5, 0.6, 0.7$, for $h = 2$.

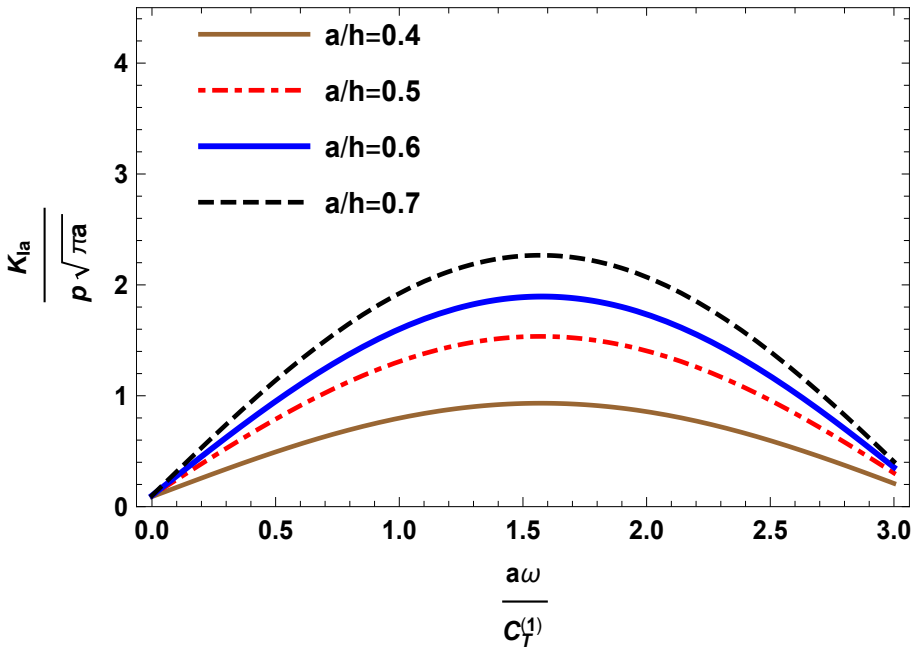

Figure 3.4: Variation of normalized K_{Ia} vs. $a\omega/C_T^{(1)}$ for problem-1 at $a/h = 0.4, 0.5, 0.6, 0.7$, for $h = 4$.

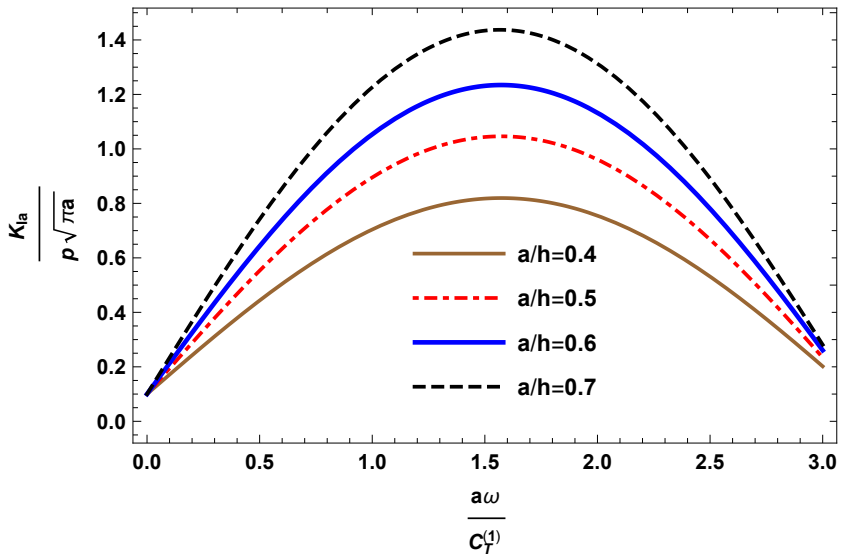

Figure 3.5: Variation of normalized K_{Ia} vs. $a\omega/C_T^{(1)}$ for problem-1 at $a/h = 0.4, 0.5, 0.6, 0.7$, for $h = 6$.

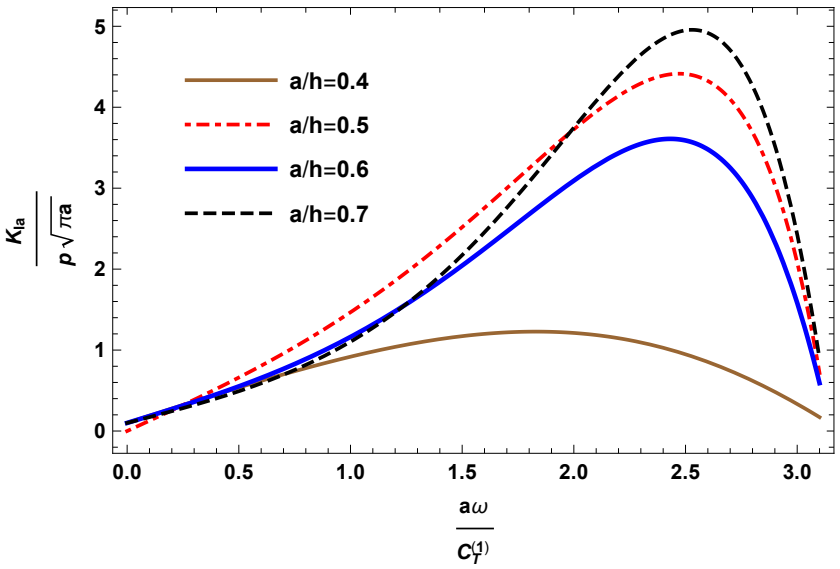

Figure 3.6: Variation of normalized K_{Ia} vs. $a\omega/C_T^{(1)}$ for problem-2 at $a/h = 0.4, 0.5, 0.6, 0.7$, for $h = 2$.

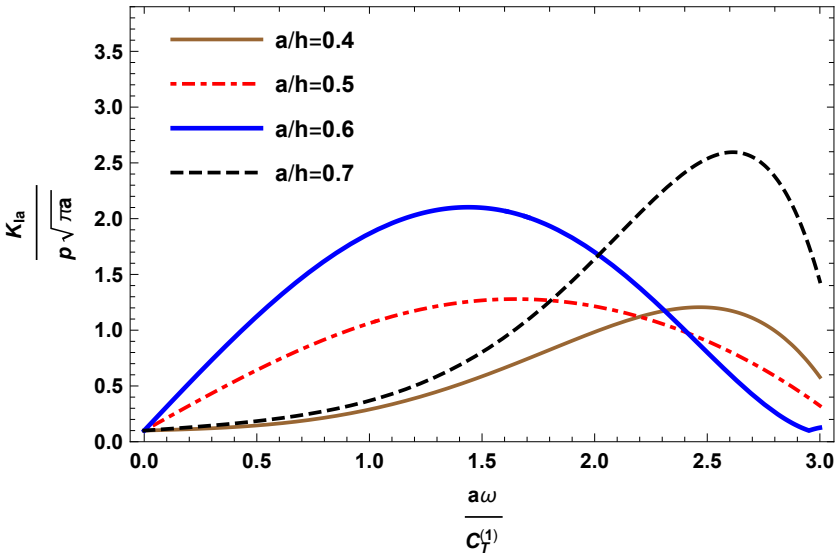

Figure 3.7: Variation of normalized K_{Ia} vs. $a\omega/C_T^{(1)}$ for problem-2 at $a/h = 0.4, 0.5, 0.6, 0.7$, for $h = 4$.

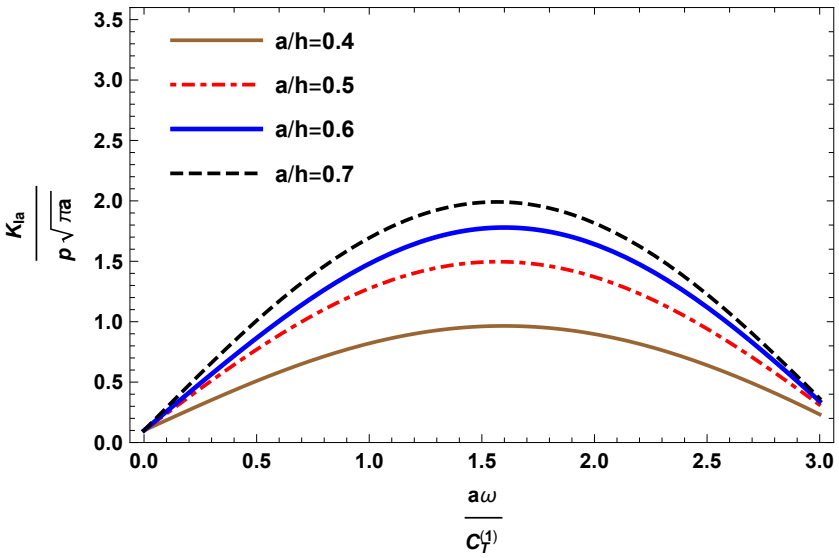

Figure 3.8: Variation of normalized K_{Ia} vs. $a\omega/C_T^{(1)}$ for problem-2 at $a/h = 0.4, 0.5, 0.6, 0.7$, for $h = 6$.

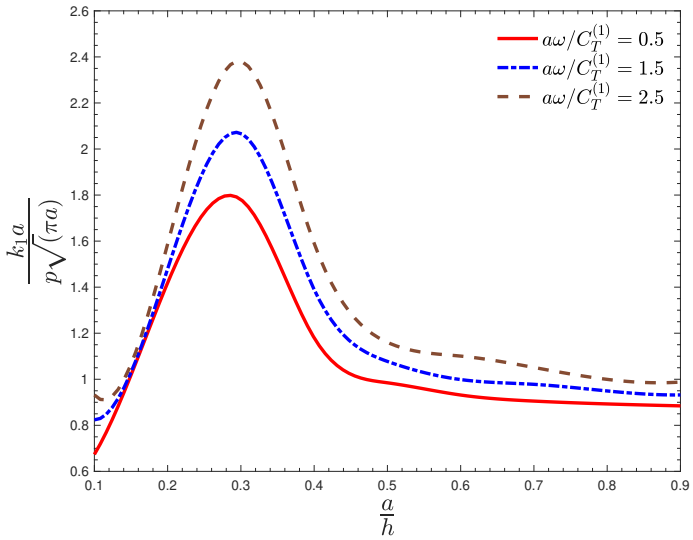

Figure 3.9: Variation of normalized K_{Ia} vs. a/h for problem-1 at $a\omega/C_T^{(1)} = 0.5, 1.5, 2.5$, for $h = 2$.

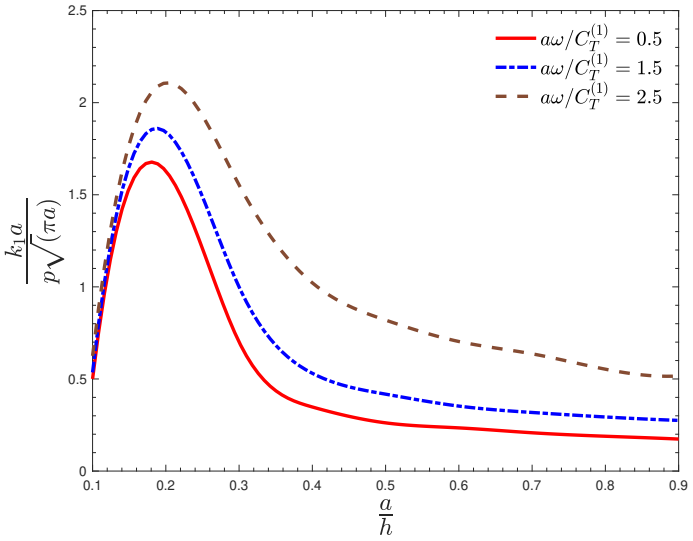

Figure 3.10: Variation of normalized K_{Ia} vs. a/h for problem-1 at $a\omega/C_T^{(1)} = 0.5, 1.5, 2.5$, for $h = 4$.

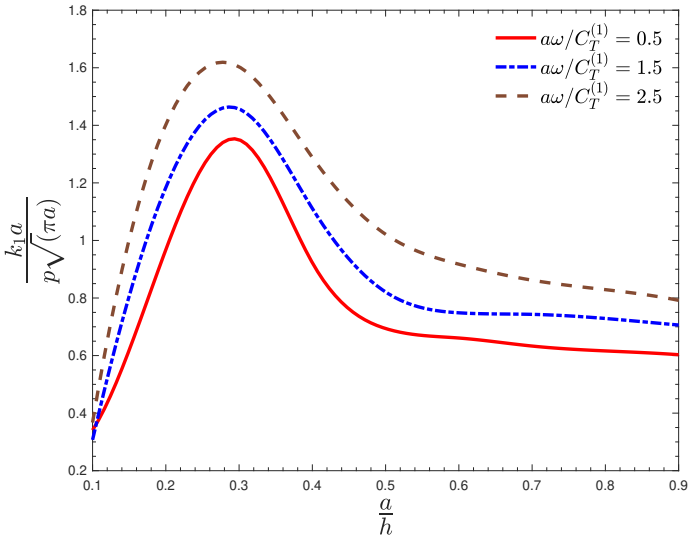

Figure 3.11: Variation of normalized K_{Ia} vs. a/h for problem-1 at $a\omega/C_T^{(1)} = 0.5, 1.5, 2.5$, for $h = 6$.

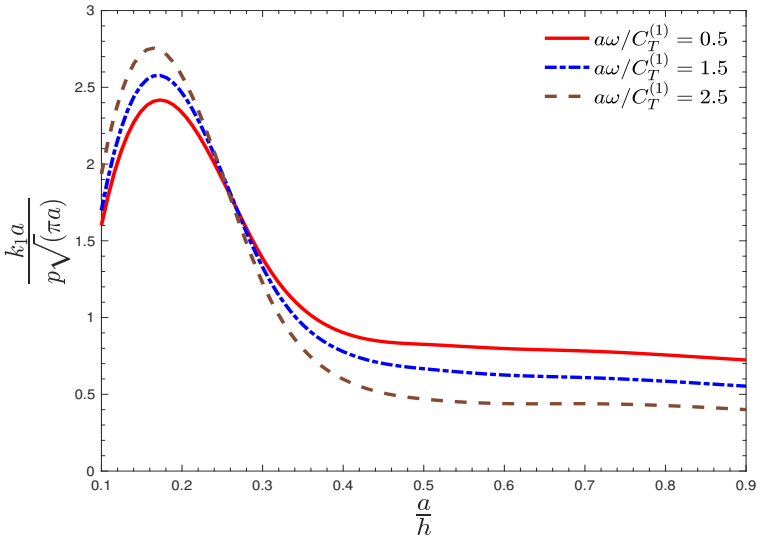

Figure 3.12: Variation of the normalized K_{Ia} vs. a/h for problem-2 at $a\omega/C_T^{(1)} = 0.5, 1.5, 2.5$, for $h = 2$.

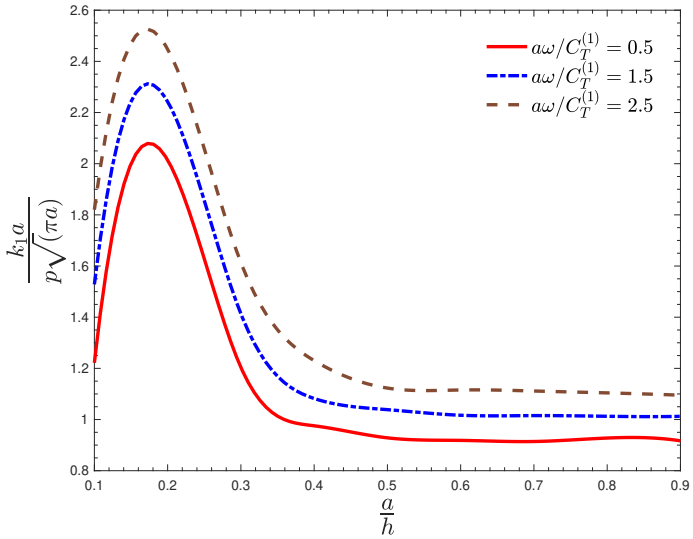

Figure 3.13: Variation of normalized K_{Ia} vs. a/h for problem-2 at $a\omega/C_T^{(1)} = 0.5, 1.5, 2.5$, for $h = 4$.

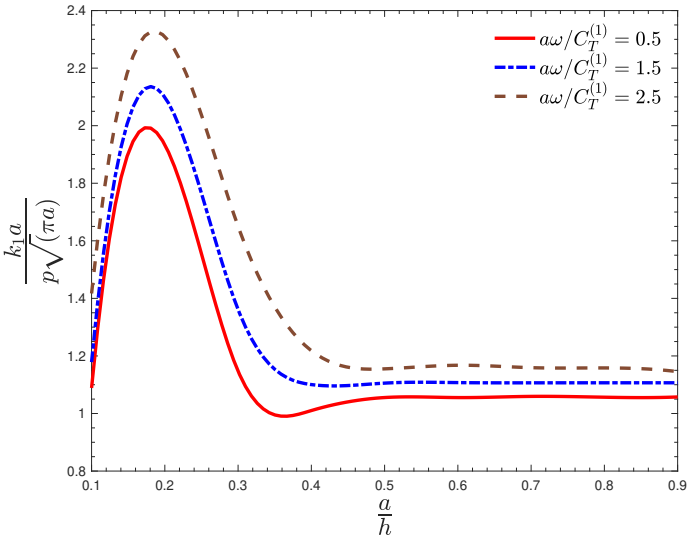

Figure 3.14: Variation of normalized K_{Ia} vs. a/h for problem-2 at $a\omega/C_T^{(1)} = 0.5, 1.5, 2.5$, for $h = 6$.

The numerical results depicted above show the effect of increment in SIF as the dimensionless quality a/h increases for Figs.[3.3]-[3.8]. The high peak can be seen for a higher value of the wavenumber, i.e., as the frequency of the time-harmonic wave increasing, SIF is increasing. This phenomenon can be seen for both the problems. For Figs.[3.9]-[3.14], the normalized SIF curves are depicted for various wave numbers, and again as the wave number is increasing, the peaks of SIF are getting higher. Both models show the same nature of increment and decrement in the curves of the normalized SIF. The increment in SIF for problem-2 is higher for every different particular cases concerning problem-1.

3.5 Conclusion

The contribution from this chapter achieves two significant goals:

- The first one is deriving the approximate analytical expression of the SIF for the edge crack for both the problems under the time-harmonic wave distribution on the crack surface.

- The second one is the graphical presentations of the normalized SIF at the crack tip $x = a$ for both the problems with respect to various wave numbers $(a\omega/C_T^{(1)})$ and also with respect to the various dimensionless quantity a/h.